



# On the crystal structures of $Ln_3MO_7$ ( $Ln = Nd, Sm, Y$ and $M = Sb, Ta$ )—Rietveld refinement using X-ray powder diffraction data

W.T. Fu\*, D.J.W. Ijdo

Leiden Institute of Chemistry, Gorlaeus Laboratories, Leiden University, P.O. Box 9502, 2300 RA Leiden, The Netherlands

## ARTICLE INFO

### Article history:

Received 25 March 2009

Received in revised form

12 June 2009

Accepted 18 June 2009

Available online 24 June 2009

### Keywords:

Crystal structure and symmetry

X-ray diffraction

Phase transition

## ABSTRACT

We have investigated, using X-ray powder diffraction data, the crystal structures of some fluorite derivatives with the formula  $Ln_3MO_7$  ( $Ln =$  lanthanide or Y and  $M = Sb$  and Ta). In these compounds ordering of  $Ln$  and  $M$  occurs, leading to a parent structure in  $Cmmm$ . Tilting of the  $MO_6$  octahedra causes doubling of one of the cubic axes, leading to a number of non-isomorphic subgroups, e.g.  $Cmcm$ ,  $Ccmm$  and  $Cccm$ . We have identified an alternative space group  $Ccmm$  instead of  $C222_1$  for those compounds containing a medium sized lanthanide or Y and  $M$  being Sb or Ta. Interestingly this is an alternative setting for the space group of the structure obtained when  $Ln$  is large ( $Cmcm$ ). However, there tilting of the octahedra is around the  $a$ -axis of the parent structure, rather than around the  $b$ -axis as it is found in the compounds which we are reporting on here.

In one compound,  $Nd_3TaO_7$ , both tilts occur. The phase transition between the two possible structures is a slow and difficult process above 80K, allowing both phases to coexist.

© 2009 Elsevier Inc. All rights reserved.

## 1. Introduction

A large number of compounds with the general formula  $Ln_3MO_7$ , in which  $Ln$  is a trivalent lanthanide or Y and  $M$  is a pentavalent metal cation, adopt a structure related to the defect-fluorite. Allpress and Rossell [1,2] have initially studied the compounds with  $M = Nb, Ta$  and  $Sb$ , and proposed three types of crystal structures. The first type crystallizes in the space group  $Cmcm$  which is found in compounds containing large lanthanides. The second one has the space group  $C222_1$ , a subgroup of  $Cmcm$ , which is adopted by lanthanides with a medium size including Y. For even smaller lanthanides, the cubic defect fluorite structure is generally observed.

The most interesting structural feature of the first two types is the ordering of  $Ln$  and  $M$  cations with the ratio of 3:1. This cation ordering together with the anion ordering of the oxygen vacancies lead to the corner-shared  $MO_6$  octahedra forming one-dimensional chains parallel to the [001] direction of the orthorhombic structure. The main difference between the two structures is, however, the tilting of the  $MO_6$  octahedra being around the axes either parallel to [100] (in  $Cmcm$ ) or to [010] (in  $C222_1$ ), respectively.

In the past years, the structural, electronic and magnetic properties of several  $Ln_3MO_7$  compounds, with  $Ln =$  lanthanide or

$Y, M = Nb, Ta, Mo, Re, Ru, Os, Ir$  and  $Sb$ , have been investigated because of their interesting one-dimensional structural property [1–18]. The existence of the first type of structure (space group  $Cmcm$ ) has been confirmed by neutron powder diffraction [4,8,10,11], X-ray powder diffraction [2,5,7,14,15,17] as well as by X-ray single crystal diffraction [13]. Of the second type, only limited X-ray powder diffraction studies were reported. Rossell [2] determined the structure of  $Y_3TaO_7$  and reported the space group  $C222_1$ . According to Allpress and Rossell [1]  $Y_3SbO_7$  has the same structure. Recently studies have been published on the compounds  $Ln_3TaO_7$  [5],  $Dy_3ReO_7$  [7] and  $Eu_3NbO_7$  [18]. However, from the refined atomic positions given in these studies, one notices that some shifts of metal atoms from the ideal position are statistically not significant. In addition, the geometry of the  $MO_6$  described in  $C222_1$  does not correspond to a tilt of the rigid octahedron: the basal oxygen atoms are not co-planar and the O–O distances of the opposite edges are either too short (e.g.  $d_{O_2-O_2} = 2.35 \text{ \AA}$  in  $Y_3TaO_7$ ) or too long ( $d_{O_1-O_1} = 3.03 \text{ \AA}$ ) [2]. These facts may suggest an inappropriate choice of space group. Furthermore, the transition from the  $Cmcm$  structure to that of the  $C222_1$  has been observed in  $Nd_3TaO_7$  [5].

In continuation of our recent works on the weberite-like  $Ca_2Ln_3Sb_3O_{14}$  [19] and the chiolite-like  $Ca_5Te_3O_{14}$  [20], we have re-investigated, using X-ray powder diffraction data, the structures occurring in the fluorite-related compounds  $Ln_3MO_7$  ( $Ln =$  lanthanide and Y;  $M = Ta$  and  $Sb$ ) with emphasis on the structures adopted by those of the medium-sized lanthanides. In this paper, we show that the space group  $C222_1$  once reported

\* Corresponding author.

E-mail address: [w.fu@chem.leidenuniv.nl](mailto:w.fu@chem.leidenuniv.nl) (W.T. Fu).

in these systems is inappropriate and the correct one is likely to be *Cmcm*. Remarkably, this space group and the unit cell are the same as those observed for large lanthanides but with different tilting direction of the  $MO_6$  octahedra. We have confirmed also that  $Nd_3TaO_7$  occurs in both *Cmcm* and *Ccm* space groups and that the *Cmcm*  $\rightarrow$  *Ccm* phase transition is sluggish due to the kinetic factors.

## 2. Experimental

Samples of  $Ln_3SbO_7$  and  $Ln_3TaO_7$ , with  $Ln = Nd, Sm$  and  $Y$ , were prepared from  $Nd_2O_3$ ,  $Sm_2O_3$ ,  $Y_2O_3$ ,  $Sb_2O_3$  and  $Ta_2O_5$  in alumina crucibles using the standard solid-state reaction.  $Nd_2O_3$  was heated at 1273 K overnight beforehand. The mixture containing  $Sb_2O_3$  was first heated overnight at 1073 K. After grinding, the resulting powder was sintered for several days at 1473 K. For the Ta compounds the sintering temperature was 1773 K. The syntheses were carried out in air and all samples were furnace cooled to room temperature.

X-ray powder diffraction data were collected on a Philips X'Pert diffractometer, equipped with the X'Celerator, using  $CuK\alpha$  radiation. For non-ambient X-ray diffraction, an Anton Paar TTK 450 chamber was used with direct sample cooling/heating in the temperature range between 80 and 723 K and a temperature stability of  $\sim 0.1$  K. The patterns were measured in the  $2\theta$  range between  $10^\circ$  and  $140^\circ$  in steps of  $0.02^\circ$  ( $2\theta$ ), counting time 10 s. The model refinements were performed by the Rietveld method using the Rietica computer program [21]. A fifth order polynomial function with six parameters was used to fit the background. The profiles were described by a pseudo-Voigt function.

## 3. Results

X-ray diffraction patterns of  $Ln_3MO_7$ ,  $Ln = Sm$  or  $Y$  and  $M = Ta$  or  $Sb$  show a C-centred orthorhombic unit cell with the cell parameters  $a \approx 2a_c$ ,  $b \approx \sqrt{2}a_c$ , and  $c \approx \sqrt{2}a_c$ , where  $a_c$  is the lattice parameter of the cubic fluorite ( $a_c \approx 5.3 \text{ \AA}$ ). Close inspection of the superlattice reflections (Fig. 1) has revealed the presence of the (201) diffraction line at  $2\theta \approx 20.7^\circ$  ruling out the space group *Cmcm* for these compounds. The structure of  $Ln_3MO_7$  with  $Ln = Sm$  or  $Y$  and  $M = Ta$  or  $Sb$  was first modelled in the space group *C222*<sub>1</sub>, as was reported in the literatures [1,2]. While all refinements did result in a reasonably low  $R_{wp}$ -value, the displacements of some metal atoms from the ideal positions in *Cmcm* were found to be insignificant with respect to their standard deviations. In the case of  $Y_3SbO_7$ , for example, the  $y$ -coordinate of Y1 is 0.5011(13). Also the refined  $z$ -coordinate of Y2 and  $y$ -coordinate of Sb are 0.0027(11) and  $-0.0051(11)$ , respectively. Furthermore, the refinement in *C222*<sub>1</sub> resulted in high values of the correlation between O1 and O2, indicating that they are possibly equivalent. These observations let us to suspect the correctness of *C222*<sub>1</sub> and to consider another space group with higher symmetry. To conserve the typical structure, i.e. the  $MO_6$  octahedra being tilted round the two-fold axes parallel to [010], as well as the observed superlattice reflections, the space group *Ccm* was chosen. To get the origin on the centre of symmetry, shifting the origin along the  $c$ -axis by  $\frac{1}{4}c$  was necessary. Consequently, the position of the  $M$  atoms is moved from the  $0, y, \frac{1}{4}$  ( $y \approx 0$ ) in *C222*<sub>1</sub> to a centre of symmetry at 000 in *Ccm*. Also the  $Ln1$  atoms are in the centrosymmetric position at  $0, \frac{1}{2}, 0$  instead of at  $0, y, \frac{1}{4}$  ( $y \approx 0.5$ ). Clearly, the new space group *C2/c2/m2<sub>1</sub>/m* is a super group of *C222*<sub>1</sub>. The  $MO_6$  octahedron described in *Ccm* is more symmetric.

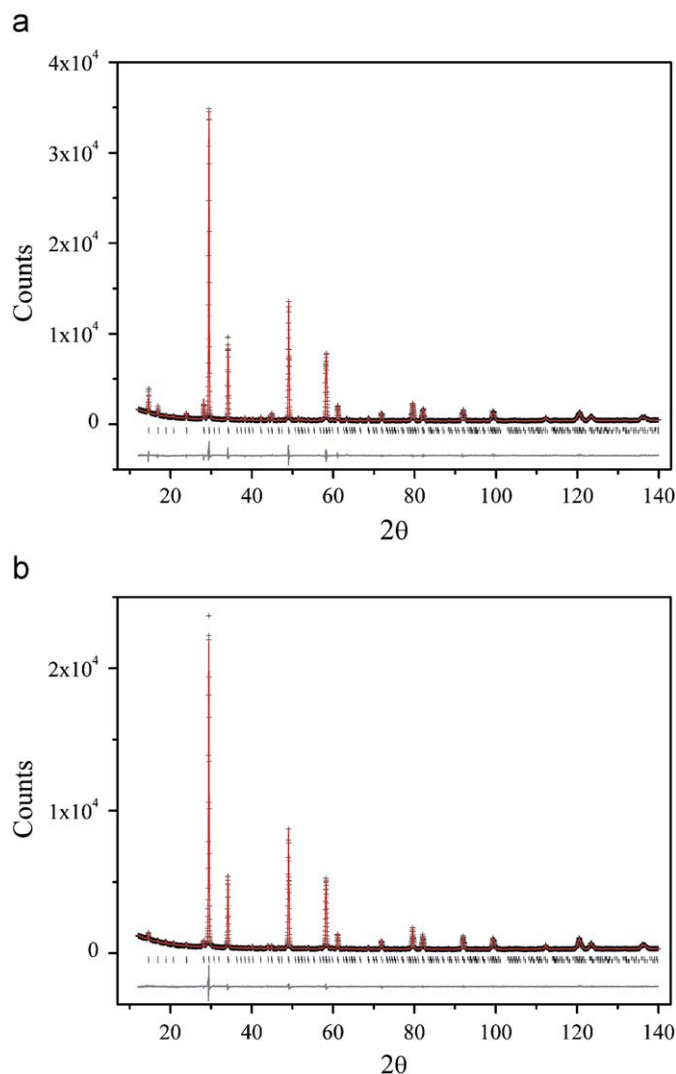


**Fig. 1.** Observed (crosses) and calculated (full line) profiles of the X-ray powder diffraction for  $Y_3TaO_7$  (a) and  $Y_3SbO_7$  in the space group *Ccm*. Tick marks below the profiles indicate the positions of the allowed Bragg reflections. A difference curve (observed–calculated) is shown at the bottom.

The Rietveld refinements carried out in *Ccm* yielded good matches between the experimental and the calculated data. In particular, the resulted agreement factors ( $R_{wp}$ ) are the same as those obtained in the space group *C222*<sub>1</sub> despite that the new model has many fewer structural parameters (8 vs. 14). Fig. 1 shows the plots of the observed and calculated profiles for  $Y_3MO_7$  ( $M = Ta$  and  $Sb$ ). The refined lattice parameters and structural parameters are given in Table 1. Table 2 lists some selected interatomic distances.

The structures that occur in  $Nd_3TaO_7$  at non-ambient temperatures were analysed in the same way. The phase transition can be easily seen by inspecting the (400) and (022) reflections. In the *Cmcm* structure these reflections separate largely and they practically merge together to a single line in the case of *Ccm* (see also discussion). In Fig. 2 we plot the evolution of the (400) and (022) reflections as the function of temperature. At room temperature, both *Cmcm* and *Ccm* phases coexist which is in agreement with the observation in the literature [5]. The coexistence of two phases persists till 80 K, the lowest temperature being reachable with the TTK450 chamber. Upon heating, the amount of the *Ccm* phase decreases and it disappears at about above 623 K. The existence of a two phase

**Table 1**  
Refined lattice parameters, atomic positions and thermal parameters of  $Ln_3MO_7$  ( $Ln = Sm$  and  $Y$ ,  $M = Ta$  and  $Sb$ ) in the space groups  $Cmcm$ .

	$Y_3TaO_7$	$Sm_3TaO_7$	$Y_3SbO_7$
$a$ (Å)	10.4857(2)	10.7109(1)	10.4843(2)
$b$ (Å)	7.4259(1)	7.53068(6)	7.4252(1)
$c$ (Å)	7.4484(1)	7.60552(5)	7.4401(1)
$Ln1$	4b (0,0,5,0)		
$B$ (Å) <sup>2</sup>	0.68(4)	0.62(9)	0.58(5)
$Ln2$	8g (x,y,0.25)		
$x$	0.2372(2)	0.2376(2)	0.2372(1)
$Y$	0.2388(2)	0.2381(2)	0.2392(2)
$B$ (Å) <sup>2</sup>	0.53(2)	0.62(4)	0.60(3)
$M$	4a (0,0,0)		
$B$ (Å) <sup>2</sup>	0.13(2)	0.15(7)	0.85(4)
$O1$	16h (x,y,z)		
$x$	0.1313(7)	0.116(1)	0.1272(8)
$y$	0.211(1)	0.196(1)	0.196(1)
$z$	-0.033(1)	-0.025(2)	-0.0352(9)
$O2$	4c (x,0,0.25)		
$x$	0.0637(1)	0.068(2)	0.070(2)
$O3$	4c (x,0.5,0.25)		
$x$	0.123(2)	0.147(3)	0.130(2)
$O4$	4c (x,0.5,0.25)		
$x$	-0.135(2)	-0.151(3)	-0.143(2)
$B^a$ (Å) <sup>2</sup>	1.5(1)	0.6(2)	0.2(1)
$R_{wp}/R_p/R_B$ (%)	6.55/4.92/2.48	4.84/3.70/3.20	5.68/4.37/1.69
$\chi^2$	2.48	1.22	1.52

<sup>a</sup> The thermal parameters of oxygen atoms are constrained.

**Table 2**  
Selected interatomic distances (Å) of  $Ln_3MO_7$  ( $Ln = Sm$  and  $Y$ ,  $M = Ta$  and  $Sb$ ).

	$Y_3TaO_7$	$Sm_3TaO_7$	$Y_3SbO_7$
$Ln1-O1$	2.561(7) × 4	2.61(1) × 4	2.638(7) × 4
$Ln1-O3$	2.27(1) × 2	2.47(1) × 2	2.30(1) × 2
$Ln1-O4$	2.34(1) × 2	2.49(1) × 2	2.39(1) × 2
$Ln2-O1$	2.391(8) × 2	2.48(8) × 2	2.437(8) × 2
	2.158(8) × 2	2.37(8) × 2	2.193(7) × 2
$Ln2-O2$	2.54(1) × 1	2.55(1) × 1	2.50(1) × 1
$Ln2-O3$	2.28(1) × 1	2.20(1) × 1	2.241(9) × 1
$Ln2-O4$	2.23(1) × 1	2.16(1) × 1	2.18(1) × 1
$M-O1$	2.100(7) × 4	1.94(7) × 4	1.989(8) × 4
$M-O2$	1.978(5) × 2	2.036(9) × 2	1.999(6) × 2

region in  $Nd_3TaO_7$  over a large temperature span shows that the  $Cmcm \rightarrow Ccmm$  phase transition exhibits strong hysteresis being typically first order phase transition.

#### 4. Discussion

The structures occurring in  $Ln_3MO_7$  are related to the cubic fluorite structure which consists of an *fcc* close packing of cations with anions occupying the tetrahedral interstices. Substitution of the cations in the fluorite lattice by  $Ln$  and  $M$  in the ratio 3:1 to form the  $MO_6$  octahedral chains is achieved by placing  $M$  atoms along the lattice diagonal in the manner of one row out of two being replaced by  $M$ , and by deleting two oxygen atoms per unit cell. To keep the  $MO_6$  octahedral chains as far as possible from each other, the fluorite-like cell is doubled in the  $a$  direction so that the second chain can be shifted over  $1/2(a+b)$ . Without octahedral tilting, the new unit cell would be orthorhombic, having the lattice parameters  $2a_c$ ,  $\sqrt{2}a_c$  and  $(\sqrt{2}/2)a_c$ , with the  $MO_6$  octahedral chains running along the  $c$  direction (see Fig. 3). The space group of this parent type is  $Cmmm$ , and the

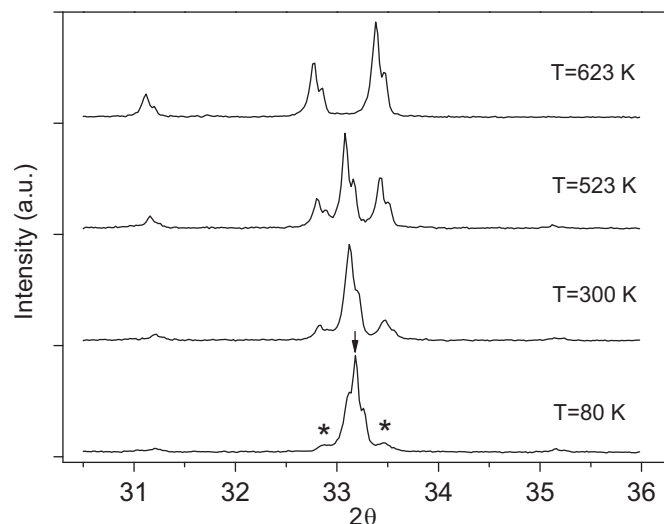


**Fig. 2.** A section of the X-ray diffraction patterns of  $Nd_3TaO_7$  showing the evolution of the (400) and (022) reflections as the function of temperature. The reflections belong to the  $Cmcm$  phase are indicated by asterisks and those of the  $Ccmm$  phase are marked by arrow.

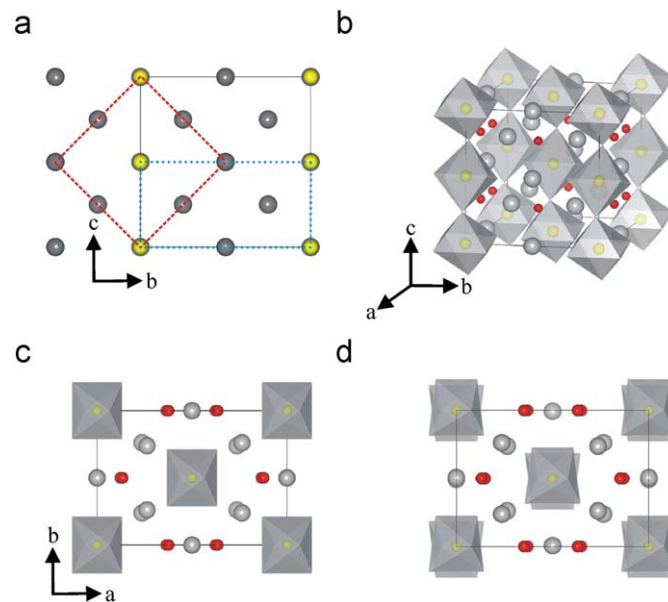


**Fig. 3.** (a) A projected view of  $Ln_3MO_7$  along the  $a$ -axis showing the ordering of  $Ln$  and  $M$  cations in the fluorite lattice. The unit cell dimensions of the fluorite, the parent  $Cmmm$  and the  $Cmcm/Ccmm$  structures are shown by dashed line, dotted line and continuous line, respectively. (b) Schematic representations of the crystal structures of  $Y_3SbO_7$  showing  $SbO_6$  octahedra and  $Y$ , Oxygens that do not bond to  $M$ -cations are also shown. (c,d) Crystal structures of  $Y_3TaO_7$  viewed along the  $c$ -axis as were refined in the space group  $Cmcm$  (this work) and  $C222_1$  [2], respectively. Note that the octahedron described in the later space group (d) is asymmetric.

corresponding atomic positions are:  $M$  in  $2a$ : 000;  $Ln1$  in  $2b$ : 00.50;  $Ln2$  in  $4f$ : 0.250.250.5;  $O1$  in  $4h$ :  $x0.5$  ( $x = 0.375$ );  $O2$  in  $8p$ :  $xy0$  ( $x = 0.125, y = 0.25$ );  $O3$  in  $2d$ : 000.5. The  $O3$  atoms take the place of oxygen atoms originally occupying the  $4h$  position (0.125,0,0.5) in the parent fluorite structure. Tilting of the  $MO_6$  octahedra doubles the  $c$ -axis giving rise to a number of non-isomorphic subgroups. In the case that the tilting is in-phase between the  $MO_6$  at (0,0,0) and at (0.5,0.5,0), the space groups are  $Cmcm$ ,  $Ccmm$  and  $Ccmm$  and the tilting parallel to [100], [010] and [001], respectively. However, if the tilting is

out-of-phase, the corresponding space groups are *Imam*, *Ibmm* and *Ibam*. Among these space groups, only *Cmcm* has been reported for  $Ln_3MO_7$ -type compounds containing a large lanthanide.

The present investigation has shown that the structure of  $Ln_3MO_7$ , with *Ln* being a medium-sized lanthanide or Y and  $M = Ta, Sb$ , is best described in the space group *Ccmm* instead of its subgroup  $C222_1$ . As was mentioned above, the refinements in  $C222_1$  did not result in any appreciable improvement. The displacements of *Ln*1 and *M* atoms from the central-symmetric positions are found insignificant with regard to the standard deviations. In fact, the X-ray diffraction patterns show the absence of the  $0kl$  reflections with  $l = 2n+1$ , e.g. the (021) reflection at  $2\theta \approx 26.9^\circ$  (Fig. 1), which are allowed in the space group  $C222_1$ . Thus the observed X-ray diffraction patterns are in agreement with the space group *Ccmm*.

In an earlier structural study [1,2], Allpress and Rossell have suggested the space group  $C222_1$  for  $Ln_3MO_7$  ( $M = Nb, Ta$  and  $Sb$ ) if *Ln* is Nd or a lower lanthanide including Y. Although they inferred from the electron diffraction patterns showing that only for  $La_3MO_7$  the reflections  $h0l$  for *l* odd were absent, no real proof has been given of  $C222_1$  being the true space group for the remaining compounds. Further, from their electron diffraction study on  $Nd_3TaO_7$  [1] it is unclear whether there is a *c* glide plane perpendicular to [100], since it is now known that two phases coexist in this compound at room temperature [5]. Therefore, one cannot invoke certain space group from these studies without criticism. In fact, in the literature the structures of  $Ln_3MO_7$  described in the space group  $C222_1$  often show quite asymmetric  $MO_6$  octahedron (see Fig. 3) and even unrealistic *M*–O bond distances. Example is shown by  $Dy_3ReO_7$ , in which the refined Re–O1 and Re–O2 distances are 2.375 and 2.434 Å, respectively [7].

The structure of  $Ln_3MO_7$  is shown by  $Y_3SbO_7$  as a representative example (Fig. 3). Y1 atoms are coordinated to eight oxygen atoms arranged in a slightly deformed cube. The averaged Y1–O distance (2.49 Å) is in agreement with the value obtained from the Shannon ionic radii (2.42 Å) (Table 2) [22]. The Y2 atom has only seven neighbouring oxygen atoms, and the  $YO_7$  polyhedron can be regarded as deformed cubic with missing oxygen. The Y2–O distances range from 2.18 to 2.50 Å with an average of 2.30 Å. This value, although being somewhat short, is expected from sum of ionic radii for the corresponding coordination number (2.36 Å). The  $SbO_6$  octahedra are tilted around the *b*-axis with the tilting angle of  $21.5^\circ$ . The averaged Sb–O distance (1.992 Å) is very close to that recently found in  $Ca_2Y_3Sb_3O_{14}$  [10], and is in good agreement with the sum of the ionic radii (2.00 Å).

It is worth noting that the structures adopted by  $Ln_3MO_7$  ( $M = Ta$  and  $Sb$ ) with large *Ln* (*Cmcm*) or medium sized *Ln* (*Ccmm*) belong to different settings of the same space group. In both structures, the chains of the  $MO_6$  octahedra are parallel to the *c*-axis. Also the *Ln*'s are coordinated with seven and eight oxygens, respectively. The main difference is, however, the tilting of the  $MO_6$  octahedra. In *Cmcm*, they tilt around the axes parallel to [100]; in *Ccmm* the tilting is around the [010] direction. Such a difference in octahedral tilting is also reflected in their X-ray diffraction patterns. For example, the *Cmcm* structure shows much large orthorhombic distortion. Particularly, tilting around the *a*-axis causes a large separation of the (400) and (022) reflections, i.e.  $d_{(400)} > d_{(022)}$ . In the case of *Ccmm*, these reflections overlap since the tilting of octahedral around the [010] direction reduces the length of the *a*-axis.

Clearly, the phase transformation in  $Ln_3MO_7$  ( $M = Ta$  and  $Sb$ ) with decreasing the size of the *Ln* cation is of a first order phase transition. This is shown by the existence of two phase region in  $Nd_3TaO_7$  over a large temperature range. In an earlier investiga-

tion [5], Wakeshima et al. showed that the *Cmcm* structure is stable at above 440 K and the " $C222_1$ " structure is stable below 170 K for  $Nd_3TaO_7$ . Between those temperatures two phases coexist. These observations have not been exactly confirmed by the present study. In fact, the *Cmcm*→*Ccmm* phase transition shows a strong hysteresis which is likely due to the hindered transition kinetics. For example, when warming up  $Nd_3TaO_7$  from a low temperature the diffraction pattern at room temperature is predominated by *Ccmm* phase. On the other hand, cooling down  $Nd_3TaO_7$  from a high temperature, the room temperature X-ray diffraction pattern shows the *Cmcm* phase as dominating phase. Furthermore, the high temperature *Cmcm* structure can be almost preserved to room temperature when  $Nd_3TaO_7$  is quenched from a high temperature, e.g. 773 K. Therefore, it is impractical to define the upper and lower temperature limits of the two phase region.

It is interesting to consider why the ideal parent structure of the space group *Cmmm* is not realized for the  $Ln_3MO_7$ -type structure. As was mentioned above, in this structure model *Ln*2 atom has only six oxygens coordinating it, and  $LnO_6$  is a highly deformed octahedron. Also, unlike the O1 and O2 atoms which are coordinated with four metal atoms, the O3 atom has just two coordinated *M*(V) metal atoms giving rise to an insufficient charge compensation on this atom. Tilting of  $MO_6$  octahedron increases the coordination number of *Ln*2 to seven. The same tilting adds also two metal atoms (*Ln*2) to the coordination sphere of O3 forming nearly a tetrahedron of oxygen. It should be mentioned that, although in both *Cmcm* and *Ccmm* structures the *Ln*2 atom has the same coordination number, the effect of the octahedral tilting is somewhat different. In the case of *Ccmm*, the tilting of  $MO_6$  octahedron brings the O3 atom closer to the *Ln*2 atom which may explain why this space group is adopted by the  $Ln_3MO_7$  compounds with smaller lanthanides.

Noteworthy is the structure of the weberite-type formula  $A_2B_2O_7$ . The weberite, e.g.  $Sr_2Sb_2O_7$  [23] and  $Ca_2Sb_2O_7$  [20], has the space group *Imma* and consists of rows of corner-linked ( $BO_6$ ) octahedra. The structure can be derived also from the defect fluorite of the parent type *Cmmm* by tilting the octahedra parallel to [100]. However, unlike the *Cmcm* structure adopted by some of the  $Ln_3MO_7$ -type compounds, in weberite the tilting of the  $MO_6$  octahedra at (0,0,0) and that at (0.5,0.5,0) is out-of-phase leading to the space group *Imam* (see the discussion above). Such out-of-phase tilting results in a clear difference between the weberite and the  $Ln_3MO_7$ -type structure. The eightfold position in the latter splits into two non-equivalent fourfold positions, one with six and one with seven coordination, respectively, to accommodate the small (*Sb*) and large (*Sr*/*Ca*) atoms. In this respect, it would be very interesting to see whether the  $Ln(III)_2M(III)M(V)O_7$ -type compound, in which *M*(III) is some small trivalent ion, can be made to adopt the weberite structure.

A related structural problem is found in  $Ln_3NbO_7$ . The space groups of these compounds were reported by Allpress and Rossell [1,2] to be *Cmcm* and  $C222_1$ , respectively. Recently, Doi et al. [18] have carried out the Rietveld refinement and found the following space groups: *Pnma* for *Ln* = La, Pr, Nd,  $C222_1$  for *Ln* = Sm–Tb and  $Fm\bar{3}m$  for *Ln* = Dy–Lu. From the refined atomic positions of  $Eu_3NbO_7$  in the space group  $C222_1$  it may be noticed that the shift in *y*- of  $Eu_1$  and *Nb* and the shift in the *z*-direction of  $Eu_2$  from the ideal positions are not significant. In the light of the present investigation, the compounds  $Ln_3NbO_7$  with *Ln* = Sm–Tb may also have the space group *Ccmm*.

In conclusion, we have re-investigated the crystal structure of some members of the  $Ln_3MO_7$ , with  $M = Ta$  and  $Sb$ , using X-ray powder diffraction data. It is shown that the structures adopted by lanthanides with a medium size as well as Y is best described in the space group *Ccmm* instead of the subgroup  $C222_1$ . The unit cell is the same as that reported for large lanthanides (*Cmcm*) but with

different tilting of the  $MO_6$  octahedra. We also confirmed that  $Nd_3TaO_7$  lies on the border between two stable phases. The coexistence of both  $Cmcm$  and  $Ccmm$  structures over an unusual large temperature range is due to the transition kinetics that hampers the phase transition.

### Acknowledgment

The authors are indebted to Dr. R.A.G. de Graaff for valuable discussions.

### Appendix A. Supplementary material

Supplementary data associated with this article can be found in the online version at [10.1016/j.jssc.2009.06.028](https://doi.org/10.1016/j.jssc.2009.06.028).

### References

- [1] J.G. Allpress, H.J. Rossell, J. Solid State Chem. 27 (1979) 105.
- [2] H.J. Rossell, J. Solid State Chem. 27 (1979) 115.
- [3] A. Kahn-Harari, L. Mazerolles, D. Michel, F. Robert, J. Solid State Chem. 116 (1995) 103.
- [4] J.F. Vente, R.B. Helmholtz, D.J.W. Ijdo, J. Solid State Chem. 108 (1994) 18.
- [5] M. Wakeshima, H. Nishimine, Y. Hinatsu, J. Phys. Condens. Matter 16 (2004) 4103.
- [6] J.E. Greedan, N.P. Raju, A. Wegner, P. Gougeon, J. Padiou, J. Solid State Chem. 129 (1997) 320.
- [7] Y. Hinatsu, M. Wakeshima, N. Kawabuchi, N. Taira, J. Alloys Compd. 374 (2004) 79.
- [8] W.A. Groen, F.P.F. van Berkel, D.J.W. Ijdo, Acta Crystallogr. C 43 (1987) 2262.
- [9] P. Khalifah, R.W. Erwin, J.W. Lynn, Q. Huang, B. Batlogg, R.J. Cava, Phys. Rev. B 60 (1999) 9573.
- [10] P. Khalifah, Q. Huang, J.W. Lynn, R.W. Erwin, R.J. Cava, Mater. Res. Bull. 35 (2000) 1.
- [11] F. Wiss, N.P. Raju, A.S. Wills, J.E. Greedan, Int. J. Inorg. Mater. 2 (2000) 53.
- [12] D. Harada, Y. Hinatsu, Y. Ishii, J. Phys. Condens. Matter 13 (2001) 10825.
- [13] W.R. Gemmill, M.D. Smith, H.-C. Zur Loye, Inorg. Chem. 43 (2004) 4254.
- [14] D. Harada, Y. Hinatsu, J. Solid State Chem. 164 (2002) 163.
- [15] J.R. Plaisier, R.J. Drost, D.J.W. Ijdo, J. Solid State Chem. 169 (2002) 189.
- [16] R. Lam, T. Langet, J.E. Greedan, J. Solid State Chem. 171 (2003) 317.
- [17] J.F. Vente, D.J.W. Ijdo, Mater. Res. Bull. 26 (1991) 1255.
- [18] Y. Doi, Y. Harada, Y. Hinatsu, J. Solid State Chem. 182 (2009) 707.
- [19] Y.S. Au, W.T. Fu, D.J.W. Ijdo, J. Solid State Chem. 180 (2007) 3166.
- [20] W.T. Fu, D.J.W. Ijdo, J. Solid State Chem. 181 (2008) 1236.
- [21] C.J. Howard, B.A. Hunter, A computer program for Rietveld analysis of X-ray and neutron powder diffraction patterns, Lucas Height Research Laboratories, 1998.
- [22] R.D. Shannon, Acta Crystallogr. A 32 (1976) 751.
- [23] W.A. Groen, D.J.W. Ijdo, Acta Crystallogr. C 44 (1988) 782.